

Growth mechanism and thermoelectric properties of PbTe/SnTe/PbTe heterostructures

E.I. Rogacheva^{a,*}, S.N. Grigorov^a, O.N. Nashchekina^a, T.V. Tavrina^a, S.G. Lyubchenko^a, A.Yu. Sipatov^a, V.V. Volobuev^a, A.G. Fedorov^b, M.S. Dresselhaus^c

^aNational Technical University “Kharkov Polytechnic Institute”, 21 Frunze Street, Kharkov 61002, Ukraine

^bInstitute for Single Crystals, 60 Lenin Av., Kharkov 61001, Ukraine

^cDepartment of Electrical Engineering and Computer Science and Department of Physics, Massachusetts Institute of Technology, 77 Massachusetts Ave., Cambridge, MA 02139-4307, USA

Received 6 January 2004; accepted 9 June 2005

Available online 14 July 2005

Abstract

An electron microscopy study of the mechanism of SnTe and PbTe layer growth in PbTe/SnTe/PbTe heterostructures prepared by thermal evaporation in vacuum onto a KCl substrate was performed. It is established that PbTe and SnTe grow on one another in a layer-by-layer fashion with the introduction of misfit dislocations on the interface at a critical thickness $d_c \approx 2$ nm. The experimentally determined dependence of the elastic stress in a growing layer (either PbTe or SnTe) on the layer thickness and the critical thickness are in good agreement with those calculated theoretically. The dependences of the thermoelectric properties of PbTe/SnTe/PbTe heterostructures on the SnTe layer thickness ($d_{\text{SnTe}} = 5–100$ nm) at fixed thicknesses of the PbTe layers were studied at room temperature. It was found that in the thickness range of $d_{\text{SnTe}} \approx (10–15)$ nm, an inversion of the dominant carrier sign from n to p takes place. The d -dependences of the thermoelectric properties were interpreted within the framework of a three-layer model, treating a PbTe/SnTe/PbTe heterostructure as three conductors connected in a parallel fashion, each characterized by its specific electrophysical parameters.

© 2005 Elsevier B.V. All rights reserved.

PACS: 73.50-h

Keywords: Lead telluride; Tin telluride; Electron microscopy; Electrical properties and measurements

1. Introduction

The theoretical prediction of the possibility of enhancing the thermoelectric figure of merit in superlattices (SL's) containing very thin layers [1–3], as well as a number of experimental demonstrations that followed [4–7], have stimulated the interest of experimentalists in studying the thermoelectric properties of heterostructures including SL's. The fulfillment of the theoretical prediction [1–3] depends to a great extent, not only on the energy band structure and the thermoelectric properties of materials, but also on structural and kinetic factors, which determine the degree

to which a real structure corresponds to a model. This determines the importance of studying mechanisms of thin layer growth, interface structure, etc.

PbTe and PbTe-based solid solutions are promising thermoelectric materials, whose thermoelectric properties have been studied in a great number of works [8–10]. At present, well-known are PbTe-based quantum-well [4–7] and quantum-dot [7,11,12] SL's in which a significant increase in thermoelectric figure of merit compared to bulk crystals has been observed. All this stimulates further studies of low-dimensional structures based on PbTe.

The objects of the present study are epitaxial thin film heterostructures PbTe/SnTe/PbTe with a size mismatch between PbTe and SnTe crystal lattices $\sim 2.2\%$ [13]. The specificity of these objects consists not only in a substantial difference in the energy band structures (PbTe and SnTe

* Corresponding author. Tel.: +7 380 572 400 092; fax: +7 380 572 400 601.

E-mail address: rogacheva@kpi.kharkov.ua (E.I. Rogacheva).

have inverted band structures relative to one another [14]) and in the electrophysical properties of the constituent layers, but also in the difference in the sign of the dominant carrier type in each of the thin layers. SnTe is a semi-conducting compound with a wide, one-sided homogeneity region, a high concentration of cation vacancies and *p*-type charge carriers ($\sim 10^{20}–10^{21} \text{ cm}^{-3}$) [13,14]. Both SnTe bulk crystals and SnTe films always exhibit *p*-type electrical conductivity [15–19]. PbTe has a narrow, two-sided homogeneity region, and can be either of *p*- or *n*-type depending on the character of the deviation from stoichiometry [13,14]. When stoichiometric PbTe is used as the charge, PbTe films of *n*-type are usually obtained [15,20–22]. Thus, one can expect that in a PbTe/SnTe/PbTe heterostructure, *p*- and *n*-type layers will coexist, and that a change in the ratio of layer thicknesses will lead to an inversion of the dominant carrier sign. That is why such a heterostructure is a convenient model for studying thermoelectric properties of low-dimensional structures with layers exhibiting *n*- and *p*-type conductivity.

In Ref. [23], for a SnTe thin film deposited on PbTe, the critical thickness, i.e. the thickness at which the introduction of misfit dislocations (MD's) in the interface starts ($d_c \approx 2 \text{ nm}$), and the elastic stress of a SnTe layer as a function of the layer thickness were both computed. It was found experimentally in the same work that in SnTe films deposited on PbTe at the substrate temperature $T_S = 625 \text{ K}$, the actual d_c is five times as large as the theoretical value of d_c , and in SnTe films whose thickness is ten times as large as the critical thickness, there remains a substantial residual elastic stress ($\sim 0.5\%$). The authors of Ref. [23] suggested that one of the reasons for the discrepancy between theory and experiment is an alloying effect, which occurs due to the relatively high substrate temperature during the evaporation, and this alloying effect can diminish the misfit of layers at the interfaces in the prepared samples. In Ref. [24], it was noted that a high temperature of deposition can lead to diffusion at the PbTe/SnTe interfaces, and the estimated width of the interdiffused interface region is about 1 nm. In Ref. [25], the galvanomagnetic properties of PbTe/SnTe SL's were studied with the period varying in the range $D = 9–33 \text{ nm}$ and with the ratio of the SnTe layer thickness to that of the PbTe layer within the period ($d_{\text{SnTe}}/d_{\text{PbTe}} \sim 1:2$ (the number of periods was 10–30). All SL's were *n*-type, although separate elements of a superlattice, such as the PbTe/SnTe two-layer structures, exhibited *p*-type conductivity. The reason for the observed difference was, however, unclear.

The goals of the present work are 1) to study the influence of the substrate temperature on the mechanism of growth of PbTe and SnTe layers and to determine the critical thickness d_c in PbTe/SnTe/PbTe heterostructures and 2) to investigate the behavior of the thermoelectric properties as a function the SnTe layer thickness in these heterostructures.

On the basis of the data obtained in this work, it has been shown that a decrease in the substrate temperature results in a shrinking of the range of thicknesses at which pseudo-

morphic growth takes place. The dependences of the elastic stress in the SnTe and PbTe layers on their thickness have been established. It has been found that an increase in d_{SnTe} up to 10–15 nm at fixed thicknesses of the PbTe layers leads to an inversion of the dominant carrier sign from *n* to *p*, and the position of the inversion point is in good agreement with theoretical calculations within the framework of a model taking into account the coexistence of conducting layers of both *n*- and *p*-type.

2. Experimental details

PbTe and SnTe thin films were grown by thermal evaporation of a PbTe and SnTe stoichiometric charge from tungsten “boats” in an oil-free vacuum ($10^{-5}–10^{-6} \text{ Pa}$) and the subsequent deposition onto (001) KCl substrates heated to $(520 \pm 10) \text{ K}$. The unit cell parameters of PbTe, SnTe, and KCl, which crystallize in a NaCl structure, are 0.646, 0.630 and 0.629 nm, respectively [13,26]. For thin film structure preparation, we used only KCl substrates of high quality, without steps. The condensation rate was 0.1–0.3 nm/s. The layer thickness and condensation rate were monitored by a calibrated quartz resonator, which was located near the substrate holder. Using the same technique, two- and three-layer heterostructures were prepared by the consecutive deposition of PbTe and SnTe layers. All films and heterostructures were covered with a 15–25 nm thick EuS layer, to protect them from oxidation. EuS layers were grown by electron-beam evaporation of europium sulfide in vacuum. In the PbTe/SnTe/PbTe heterostructures, the thicknesses of the lower (buffer) and upper PbTe layers were kept fixed and equaled $d_{1,\text{PbTe}} \approx 40 \text{ nm}$ and $d_{2,\text{PbTe}} \approx 10 \text{ nm}$, respectively. The thickness of the SnTe layer was varied in the range $d_{\text{SnTe}} = 5–100 \text{ nm}$.

The transmission electron microscopy (TEM) study was carried out using an EM-125 K electron microscope. To prepare samples for the electron microscopy study, films were separated from their substrates in distilled water and were caught on copper grids. Films whose thickness was smaller than 10 nm were fixed by a thin carbon film before separation from their substrates. The film structure was studied by the diffraction contrast technique and Moiré method in both bright- and dark-field regimes. From the dark-field images, the Burgers vector of the MD's (misfit dislocations) was determined. Moiré patterns were used to control the mismatch between the crystal lattices of different layers, to determine the mosaic structure of the films, and to identify pores in one of the layers (by the disappearance of Moiré stripes in some areas). The electron microscopy study was carried out both on (001)KCl/PbTe/SnTe/PbTe heterostructures and on PbTe/SnTe and SnTe/PbTe two-layer structures. In the case of two-layer structures, the upper layer grown on a thick lower film ($d \sim 200–400 \text{ nm}$) was wedge-shaped in cross-section, so that its thickness changed continuously from 0 to the maximum value. This structure

allowed us to study the growth mechanism and film structure at different thicknesses for a single sample.

The Hall coefficient R_H and electrical conductivity σ were measured by a conventional *dc*-method in a constant magnetic field ~ 1 T. The error of measuring R_H and σ did not exceed 5%. The Seebeck coefficient S was determined with regard to copper by a compensation technique with accuracy not worse than 3%. The effective Hall mobility of charge carriers μ was calculated as $\mu = R_H \cdot \sigma$.

3. Results

Although the fact that IV–VI chalcogenides grow by the Volmer–Weber mechanism on dielectric substrates, such as KCl, NaCl, etc. is well-known [26,27], the conditions of the epitaxial growth depend significantly on the technological parameters (substrate temperature, condensation rate, etc.) and on the real structure of the substrate surface. That is why as a first step, we studied the growth mechanism and the structure of the PbTe and SnTe films on the (001) KCl surface. Electron microscopy studies showed that PbTe and SnTe films grow in an island-like fashion on (001) KCl according to the vapor–crystal mechanism, without coalescence of islands for PbTe and with a partial coalescence of islands for SnTe. PbTe and SnTe films are continuous at $d \sim 10$ nm. Electron diffraction studies showed that the PbTe and SnTe films grow epitaxially and are monocrystalline. The predominant defects in the PbTe and SnTe films grown on (001) KCl were threading dislocations perpendicular to the film surface, which were formed in the process of the overgrowing of channels in the film. These results are similar to our results reported earlier in Refs. [22,28].

As the second step, we studied how the structure of the interface in the PbTe/SnTe and SnTe/PbTe two-layer films changes with increasing thickness of either the SnTe layer (d_{SnTe}) deposited on a thick PbTe film or the PbTe layer (d_{PbTe}) deposited on a thick SnTe film. In Fig. 1, the TEM images obtained for different sections of the wedge-shaped PbTe/SnTe film with the maximum thickness of the SnTe layer 15 nm are presented. At small thicknesses of a growing film, pseudomorphic growth takes place, but at larger thicknesses, MD's appear in the interface. First, small

segments of MD's oriented along the [110] and $[1\bar{1}0]$ are formed (Fig. 1a). As d_{SnTe} increases, these segments extend and new ones appear. The density of MD's increases evenly all over the interface, the regularity of the MD network becomes higher (Fig. 1b), and eventually at $d_{\text{SnTe}} \sim 15$ nm, a quite regular square network of MD's is formed (Fig. 1c). The character of the change in the interface structure corresponds to the layer-by-layer growth mechanism (the Frank–Van der Merwe mechanism). Similar changes in the interface structure are observed when PbTe grows on a SnTe surface. On the basis of the fact that the MD network was regular over a large area of the interface and did not contain defects in the form of torn (or shifted relative to one another) MD dislocation rows, one could conclude that there were no rough defects in the interface, and the interface was quite smooth.

It was established that MD's are edge dislocations with their Burgers vectors oriented along $\vec{b} = \frac{a}{2}[110]$, which lie in the interface plane. Both orthogonal systems of dislocations can be observed in the $\vec{g} = 200$ ($\vec{g} \cdot \vec{b} = 1$) reflection and one of the systems cannot be seen in the $\vec{g} = 220$ reflection (for which $\vec{g} \cdot \vec{b} = 0$). To fully accommodate the mismatch f of the crystal lattices at the interface in the PbTe/SnTe system, the period of the MD network should be [29]

$$D_H = \frac{b}{f}, \quad (1)$$

where

$$f = \frac{a_2 - a_1}{a_1}, \quad (2)$$

and a_1 and a_2 are the unit cell parameters of SnTe and PbTe, respectively.

The Burgers vector of MDs is a translation vector of a so-called average lattice which is formed as a result of stress relaxation at interfaces with a small crystal lattice mismatch. The period of this average lattice is determined by the equation

$$\tilde{a} = \frac{a_1 + a_2}{2} \quad (3)$$

Taking this into consideration, we obtain from Eqs. (1) and (2) that the mismatch between the PbTe and SnTe

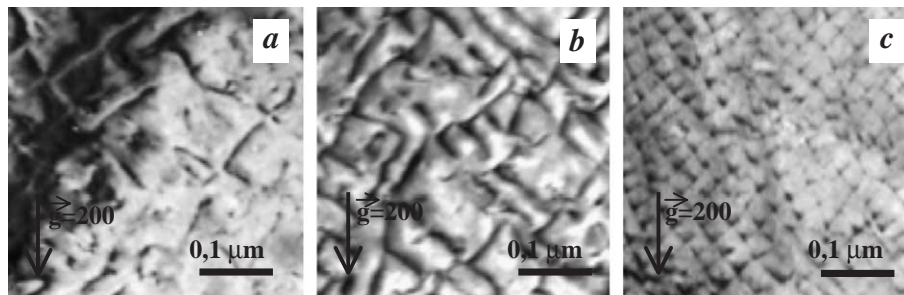


Fig. 1. The dislocation structure of the interface in the PbTe/SnTe two-layer system with a variable thickness of the SnTe layer in different sections of the wedge: (a) $d_{\text{SnTe}} = 5.5$ nm; (b) $d_{\text{SnTe}} = 10.0$ nm; (c) $d_{\text{SnTe}} = 15.0$ nm.

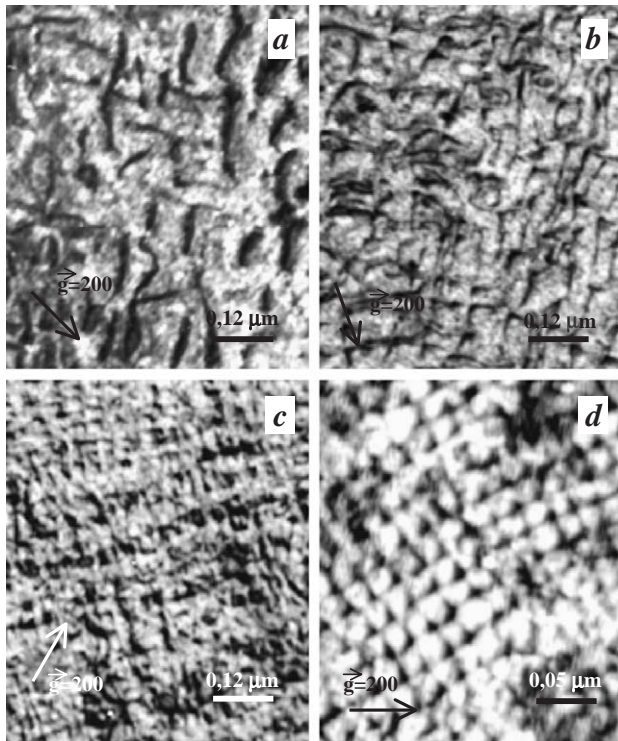


Fig. 2. The dislocation structure of the PbTe/SnTe and SnTe/PbTe interfaces in the (001)KCl/PbTe/SnTe/PbTe/EuS heterostructures. (a) $d_{\text{SnTe}}=2.8$ nm; (b) $d_{\text{SnTe}}=5.5$ nm; (c) $d_{\text{SnTe}}=16.5$ nm; (d) $d_{\text{SnTe}}=36.6$ nm.

crystal lattices is 2.06% and the equilibrium value of the period of the MD network is $D_{\text{H}} \cong 22$ nm. It is established experimentally that in the PbTe/SnTe heterosystem, at $d_{\text{SnTe}} \geq 15$ nm, the period of the MD network is $D_{\text{H}} \cong 24$ –25 nm, which in contrast with the results of Ref. [23], is very close to the calculated value and indicates that MD's almost fully accommodate the mismatch between the crystal lattices. We did not determine the critical thickness h_{c} of the SnTe (or PbTe) film, at which MDs start to appear, for PbTe/SnTe and SnTe/PbTe two-layer structures. When growing those structures, we continuously varied the thickness of the upper film from zero up to 40 nm. The goal was to check whether SnTe grows on PbTe (and vice versa) in a layer-by-layer fashion under our experimental conditions. According to our rough estimate, h_{c} did not exceed 3–4 nm.

In PbTe and SnTe, which crystallize in a rock-salt structure but have predominantly covalent type of bonds, the main glide planes are $\{100\}$ and $\{111\}$. That is why the introduction of MD's with the above specified Burgers vector into the (001) interface can take place only by the diffusion mechanism. On the surface of a growing epitaxial layer, a prismatic half-ring dislocation originates and then expands by climbing in the (110) plane and enters the interface. A segment of a prismatic dislocation, which is located in the interface represents a section of an edge MD. A diffusion mechanism for the introduction of MD's in the interface from the surface of an epitaxial layer was observed

in heterostructures such as GeTe/PbTe, PbSe/PbS, and many others [29].

As the third step, a TEM study of the interface structure in KCl/PbTe/SnTe/PbTe/EuS multilayered films with various SnTe layer thicknesses was performed (Fig. 2). It was established that in the PbTe/SnTe and SnTe/PbTe interfaces, separate segments of edge MD's with $\vec{b} = \frac{a}{2} [110]$ appear only for SnTe thicknesses greater than $d_{\text{SnTe}}=1.8$ nm. At smaller thicknesses of the SnTe layer, it grows pseudomorphically. Already for d_{SnTe} in the range $d_{\text{SnTe}}=2.8$ to 5.5 nm, fragments of a square network of MD's appear (Fig. 2a,b), and at $d_{\text{SnTe}}=16.5$ nm, on each interface, practically an equilibrium square network of edge MD's with a period $D_{\text{H}} \cong 25$ nm is formed (Fig. 2b). Notable is the unusual contrast in the images of many of the MD's (Fig. 2a,b): their images are wider than usual, and when the condition $\vec{g} \cdot \vec{b} = 1$ holds, the dislocations are imaged as double lines. The authors of Ref. [30], who observed similar peculiarities in the contrast of MD's when studying PbS/PbSe/PbS three-layer heterostructures, suggested that these effects are connected with the fact that in both interfaces, two segments of one prismatic dislocation loop are located exactly under one another, and they proposed a corresponding mechanism for the introduction of MD's in the second interface. The third epitaxial layer inherits all threading dislocations of the second epitaxial layer, including vertical "tails" of prismatic half-ring dislocations from the first interface. As the sign of the lattice mismatch at the second interface reverses, these "tails" climb toward one another in the third growing layer under the effect of elastic stresses. It is due to this that fragments of MD's are formed in the second interface. Since vertical "tails" of a prismatic half-ring dislocation move in the same plane of the (110) type and have opposite signs, they annihilate when meeting one another. The closing of a prismatic half-ring dislocation leads to the formation of a prismatic dislocation loop with two opposite segments located in two interfaces. Simultaneously, new prismatic half-ring dislocations originate on the free surface of the growing film. They extend due to climbing into the interface, thereby introducing segments of

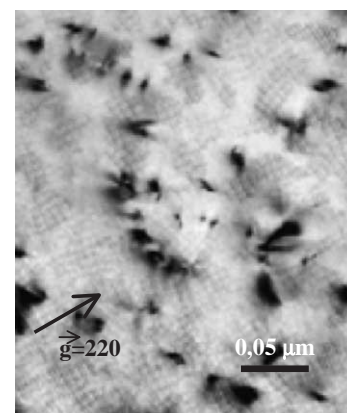


Fig. 3. The dislocation structure of the PbTe/EuS interface in the (001)KCl/PbTe/SnTe/PbTe/EuS heterostructures ($d_{\text{SnTe}}=1.1$ nm, $d_{\text{EuS}}=7$ nm).

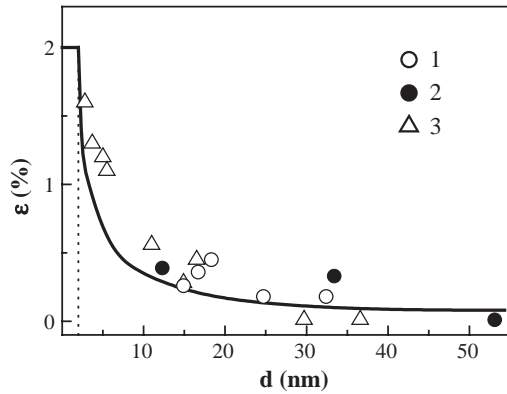


Fig. 4. Experimental (points) and theoretical [23] (curve) dependences of the deformation ε in SnTe and PbTe layers, grown on one another, on their thickness d . 1—PbTe/SnTe; 2—SnTe/PbTe; 3—PbTe/SnTe/PbTe.

new MD's in this interface. Joining already existing dislocations, these dislocations eventually form a square dislocation network. The smaller the distance between MD's and, hence, the greater the interaction between them, the higher the probability that dislocations in opposite interfaces are located exactly under one another.

Using heterostructures as objects with a very thin intermediate SnTe layer, whose thickness is less than the

critical thickness and both PbTe/SnTe and SnTe/PbTe interfaces are free of MD's, makes it possible to investigate the structure of the (001) PbTe/EuS interface. As is seen from Fig. 3, dislocations perpendicular to the film surface pierce through the entire heterostructure, and a square network of edge MDs with Burgers vector of the $\rightarrow b = \frac{a}{2} [110]$ type that belong to the (001) PbTe/EuS interface, are observed. The period of the MD network is $D_H \cong 6$ nm, which is in good agreement with the calculated value ($D_H = 5.6$ nm), obtained assuming a full accommodation of the mismatch ($f = 8.07\%$) between the PbTe and EuS crystal lattices ($a_{\text{EuS}} = 0.597$ nm [31]). This, in turn, means that the upper PbTe layer is in a non-stressed state. The EuS layer has a mosaic structure which is well-identified by distortions of the general picture of the MD distribution. A mosaic structure of the EuS layer is connected with an island-like growth of EuS on the PbTe surface. When an island-like growth takes place and there is a sufficiently large mismatch of crystal lattices of adjacent layers, MD's originate easily on the island periphery and enter a (001) interface by sliding. In this case, MD's form a regular square network in the island body, and in the locations of island coalescence, distortions of the MD network occur.

On the basis of the MD network period, the dimensionless elastic stress ε of the intermediate SnTe layer as a

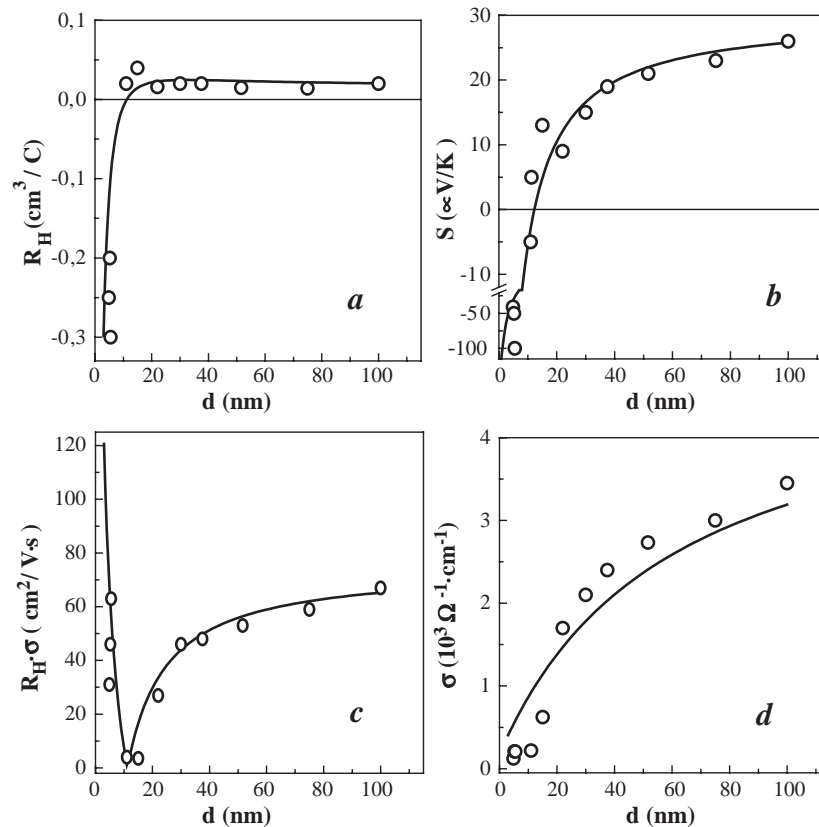


Fig. 5. Room temperature dependences of the Hall coefficient R_H (a), the Seebeck coefficient S (b), the charge carrier mobility μ (c), and the electrical conductivity σ (d) on the SnTe layer thickness d_{SnTe} in (001)KCl/PbTe/SnTe/PbTe/EuS heterostructures. The curves are the results of the theoretical calculations of d_{SnTe} -dependences on the basis of a three-layer model.

function of its thickness is calculated using the equation [29]:

$$\varepsilon = f - \frac{b}{D_H} \quad (4)$$

Since at small thicknesses of the intermediate SnTe layer, MDs are located in the interface rather irregularly, we calculated the period of the MD network as an average of 50 measurements of distances between dislocations for an experimental determination of ε . The results of the determination of ε , based on experimental data for the multilayer KCl/PbTe/SnTe/PbTe/EuS and for the two-layer KCl/PbTe/SnTe and KCl/SnTe/PbTe structures, are presented in Fig. 4. In the same figure, the theoretical curve for the PbTe/SnTe two-layer composition computed in Ref. [23] on the basis of the theoretical model for a thin film grown on a semiinfinite crystal [32] is given. Under such conditions, only the epitaxial layer is stressed. Circles in Fig. 4 correspond to elastic stress in the SnTe layer in the PbTe/SnTe two-layer structure, while triangles show elastic stress in the SnTe layer in the PbTe/SnTe/PbTe/Eus multilayer structure.

It is seen that in the multilayer structure, the introduction of MD's in the interface starts at the critical thickness of the SnTe layer ~ 2 nm, which practically coincides with d_c theoretically calculated for a two-layer structure [23]. However, with increasing thickness of the SnTe layer, elastic stresses in the intermediate layer decrease, but not so rapidly as the theory predicts. At a thickness of ~ 10 nm, the elastic stress in the layer is by approximately 0.2% larger. This indicates that the introduction of MD's in the interface is hampered. At $d_{\text{SnTe}} > 15$ nm, the experimental values of ε approach the theoretical values, and the elastic stress in the SnTe layer in a multilayer structure becomes practically similar to the stress in a two-layer system.

In Fig. 5, the dependences of the Hall coefficient, the Seebeck coefficient, the charge carrier mobility, and the electrical conductivity on the SnTe layer thickness in PbTe/SnTe/PbTe heterostructures are shown. It is seen from the figure that when starting at very small d_{SnTe} , R_H and S decrease in absolute value with increasing SnTe layer thickness, and in the vicinity of $d_{\text{SnTe}} \sim 10$ –15 nm, the inversion of the dominant carrier sign from n to p takes place. In the specified interval of thicknesses, the dominant carrier sign is unstable, and is very sensitive to a change in thickness and to the conditions of growth. Near the inversion point, the effective charge carrier mobility has its minimum, and then it sharply increases up to $d_{\text{SnTe}} \sim 30$ nm, and after that μ increases slightly. Starting from $d_{\text{SnTe}} \sim 20$ nm, the Hall coefficient R_H remains practically the same, while the Seebeck coefficient increases up to the values that are usually observed in sufficiently thick SnTe films. A sharp increase in electrical conductivity is observed after it changes its type from p to n .

4. Discussion

Thus, it follows from the results obtained in this work that in PbTe/SnTe/PbTe heterostructures, PbTe and SnTe grow on one another in a layer-by-layer fashion with the formation of MDs at the critical thickness $d_c \cong 2$ nm. The difference between the experimentally obtained and theoretically computed dependences of elastic stress ε in the intermediate SnTe layer on its thickness can be connected with the fact that in a multilayer structure with layers of comparable thicknesses, not only the intermediate SnTe layer but also the adjacent PbTe layers are stressed. The kinetics of the introduction of MD's in both interfaces depends on the stressed states of all three layers. The fact that, in spite of the difference between the model assumptions [23,32] and the actual situation, practically ideal coincidence of the theoretically computed and experimentally determined critical thickness is observed, allows us to suggest that the simultaneous action of both factors which determine the difference between the experimental and model conditions, i.e. the presence of elastic strains in the buffer PbTe layer and the presence of the upper PbTe layer, has a compensating effect and makes the experimental conditions closer to the model ones.

It is seen from the obtained data that, as was expected, the decrease in the substrate temperature from 625 K [23] to 530 K (the present work) leads to a decrease in the value of the critical thickness to $d_c \cong 2$ nm, compare to $d_c \cong 10$ nm observed in Ref. [23]. It follows from here that an increase in the diffusion rate with increasing substrate temperature can actually lead to the formation of a solid solution at the PbTe/SnTe interface and thus to a decrease in the degree of structural mismatch between the layers. The fact that the value of d_c obtained experimentally in this work practically coincides with the theoretically calculated value shows that, under the given growth conditions, diffusion does not make any noticeable contribution to the processes taking place at the interface. These results provide additional evidence that the substrate temperature is an important parameter, which determines not only the degree of structural perfection, but also the growth mechanism.

The observed d -dependences of σ , S , and R_H can be interpreted within the framework of a simple model in which a PbTe/SnTe/PbTe heterostructure is considered as a three-layer sandwich with a large surface area and a small thickness. It is assumed that charge is transferred by electrons and holes moving along the film surface and the properties can vary perpendicular to the surface but not parallel to the surface. This sandwich consists of two identical layers of PbTe with n -type electrical conductivity and a SnTe layer exhibiting p -type conductivity and located between the PbTe layers. Each layer in the heterostructure is characterized by certain electrophysical parameters. Their contributions to the electrical conductivity are determined by the relative thicknesses of the layers. Assuming a conventional experimental configuration, corresponding to

the magnetic field perpendicular to a broad area of the sample and assuming that such a three-layer structure will behave like three power sources connected in parallel, one can obtain equations for calculating the resulting Hall coefficient, electrical conductivity and the Seebeck coefficient [33]:

$$R_H = \frac{d(\mu_p \sigma_p d_p - \mu_n \sigma_n d_n)}{(\sigma_p d_p + \sigma_n d_n)^2}, \quad (5)$$

$$\sigma = \frac{\sigma_p d_p + \sigma_n d_n}{d}, \quad (6)$$

$$S = \frac{S_p \cdot \sigma_p \cdot d_p - S_n \cdot \sigma_n \cdot d_n}{\sigma_p \cdot d_p + \sigma_n \cdot d_n}, \quad (7)$$

where the p and n subscripts refer to p - and n -type layers with thicknesses d_p and d_n , respectively, (where $d = d_p + d_n$). Under an increase in d_{SnTe} , the contribution by the p -type charge carriers becomes more significant. This leads to a decrease in R_H and S in absolute value and a subsequent inversion of the dominant carrier sign from n to p for d_{SnTe} , above the critical value of $d_{\text{SnTe}} \cong 10\text{--}15$ nm (Fig. 5a,b). The coexistence of carriers with different signs results in non-uniformity of the potential profile, especially in the inversion range, and in the corresponding decrease in μ . In the range of d_{SnTe} within this inversion range, a very deep minimum in the $\mu(d)$ dependence is observed (Fig. 5c).

The simplest estimates of the ratio of PbTe and SnTe layer thicknesses (d_n/d_p) at which the inversion of the dominant carrier sign from n to p must take place were made using Eqs. (5) and (7) ($d_n/d_p = (\mu_p \sigma_p)/(\sigma_n \mu_n)$ and $d_n/d_p = (S_p \sigma_p)/(S_n \mu_n)$ from Eqs. (5) and (7), respectively) and yielded the value $d_n/d_p = 4\text{--}6$, which is in good agreement with the d_n/d_p , ratio corresponding to the experimentally observed d_n/d_p value at the inversion point. The S , σ , and μ values for each layer ($S_p = 25\text{--}30$ $\mu\text{V/K}$, $S_n = 175\text{--}200$ $\mu\text{V/K}$, $\sigma_p = 5000\text{--}6000$ $\Omega^{-1}\text{cm}^{-1}$, $\sigma_n = 150\text{--}175$ $\Omega^{-1}\text{cm}^{-1}$, $\mu_n = 350\text{--}400$ $\text{cm}^2/\text{V s}$ and $\mu_p = 50\text{--}75$ $\text{cm}^2/\text{V s}$) were the corresponding values for thick SnTe and PbTe films prepared in the present work under identical conditions, as well as the values reported in Refs. [22,34]. It was assumed that these values were not very different from those for thinner layers due to the realization that for a layer-by-layer growth mechanism there are no apparent reasons for forming additional volume defects. Possible size effects, that can cause an oscillatory behavior of the thickness dependences of properties, were not taken into account because of our predominant interest in the monotonic components of the dependences of the thermoelectric parameters. Since the measurements were carried out on heterostructures with $d_{\text{SnTe}} > 5$ nm, we also ignored changes in energy band parameters, and, consequently, in the kinetic properties which occur during the stage of pseudomorphic growth as a result of the appearance of

elastic stresses caused by the mismatch of PbTe and SnTe crystal lattices.

In Fig. 5 the curves are the results of the theoretical calculations of d_{SnTe} -dependences of the thermoelectric and galvanomagnetic properties of PbTe/SnTe/PbTe heterostructures on the basis of a three-layer model. It is seen that there is good agreement between the experimental data and the results of theoretical calculations. It is possible to suggest that the formation of misfit dislocations, leading to the relaxation of elastic stresses at the interface determines to a certain degree the applicability of the model that allows one to consider a heterostructure to consist of independent layers of their parent bulk materials, utilizing their bulk electro-physical parameters.

Since the location of the inversion point essentially depends not only on the ratio of the constituent layer thicknesses but also on charge carrier mobility in each layer, which is very sensitive to the presence of different types of defects in thin films (pores, cracks, steps, etc.), there is a certain interval of thicknesses ($d_{\text{SnTe}} \cong 10\text{--}15$ nm) in which the dominant carrier sign is unstable.

The ratio of thicknesses at which an inversion of the dominant carrier sign occurs depends also on the charge carrier concentrations in the PbTe and SnTe layers, which, in turn, depend on the charge carrier concentration in the charge used for evaporation. As far as SnTe is concerned, regardless of the composition of the charge used for the film preparation (49–51 at.% Te), in sufficiently thick layers, the concentration of holes usually corresponds to the concentration observed in bulk stoichiometric SnTe ($p \sim (2\text{--}4) \cdot 10^{20}$ cm^{-3} [13,34]). Conversely, the electron concentration in thick PbTe films significantly depends on the initial charge composition [35]. Thus, one can expect, for instance, that with increasing charge carrier concentration in the PbTe charge, the inversion point will shift to higher thicknesses of the SnTe layer, i.e. in the direction of decreasing d_n/d_p . That is why the fact that the PbTe/SnTe SL's studied in Ref. [25], where the ratio of the SnTe and PbTe layer thicknesses in a period was $d_{\text{SnTe}}/d_{\text{PbTe}} = 1/2$, exhibited n -type conductivity can be easily explained taking into consideration that in the thick PbTe films grown in that work [25], the electron concentration reached 10^{19} cm^{-3} . The observation of p -type conductivity in PbTe/SnTe two-layer structures with the same ratio $d_{\text{SnTe}}/d_{\text{PbTe}}$, also reported in the same work [25], could be connected with oxidation processes taking place on the film surface, which was unprotected from the air. Oxygen acts as an acceptor, causing the appearance of p -type charge carriers. As we showed in Refs. [35,36], surface oxidation significantly affects the kinetic coefficients of thin n -PbTe films and this effect should be taken into account when interpreting the galvanomagnetic and thermoelectric properties of these films. In the PbTe/SnTe SL's studied in Ref. [25], probably only the upper layer was exposed to oxidation, while the conductivity type of the whole superlattice remained unchanged.

5. Conclusions

Thermal evaporation in vacuum on KCl substrates was used to prepare two-layer (PbTe/SnTe and SnTe/PbTe) and three-layer (PbTe/SnTe/PbTe) heterostructures covered with EuS. The TEM study showed that SnTe and PbTe grow on one another in a layer-by-layer fashion. At the critical thickness of the growing layer $d_c \sim 2$ nm, misfit dislocations are introduced in the interface by a diffusion mechanism due to the climbing of the dislocations. The dependence of the elastic stresses in the SnTe or PbTe layer on the layer thickness in a PbTe/SnTe/PbTe heterostructure was established experimentally and found to be in good agreement (as well as the value of the critical thickness) with the theoretically computed prediction for the two-layer PbTe/SnTe structure for the case of a thin epitaxial film growing on a semiinfinite crystal. It is suggested that the fact that elastic stress in the SnTe layer turned out to be $\sim 0.2\%$ higher than the computed one is connected with the difference in the stressed state of the SnTe layer in the three-layer heterostructure as compared to the two-layer one. The comparison of the results obtained in the present work and those reported in Refs. [23,25] showed that a decrease in the substrate temperature leads to a shrinking of the range of thicknesses at which pseudomorphic growth occurs. This proves the suggestion made in Ref. [23] about the possibility of the manifestation of alloying effects in PbTe/SnTe heterostructures at a sufficiently high substrate temperature, which lead to an increase in the critical thickness d_c .

The thermoelectric and galvanomagnetic properties of PbTe/SnTe/PbTe heterostructures were studied as a function of the SnTe layer thickness at fixed thicknesses of PbTe layers. An inversion of the dominant carrier sign (from n to p) was detected at the thickness $d_{\text{SnTe}} \sim 10\text{--}15$ nm. Within this inversion range, a minimum in the $\mu(d)$ dependence is observed. Using a “sandwich” model consisting of parallel layers of SnTe and PbTe with their bulk electrophysical parameters, the theoretical calculation of the d_{SnTe} -dependences of the thermoelectric and galvanomagnetic properties of the PbTe/SnTe/PbTe heterostructures and the estimate of the inversion point location have been carried out. It was found that theoretical calculations are in good agreement with the experimental data.

Acknowledgments

The authors thank Dr. Gene Dresselhaus for fruitful and stimulating discussions. This work was supported by the U.S. Civilian Research and Development Foundation (#UP2-2426-KH-02).

References

- [1] L.D. Hicks, M.S. Dresselhaus, Phys. Rev., B 47 (1993) 12727.
- [2] L.D. Hicks, M.S. Dresselhaus, Phys. Rev., B 47 (1993) 16631.

- [3] L.D. Hicks, T.C. Harman, M.S. Dresselhaus, Appl. Phys. Lett. 63 (1993) 3230.
- [4] L.D. Hicks, T.C. Harman, X. Sun, M.S. Dresselhaus, Phys. Rev., B 53 (1996) R10493.
- [5] T.C. Harman, D.L. Spears, M.J. Manfra, J. Electron. Mater. 25 (1996) 1121.
- [6] T.C. Harman, D.L. Spears, M.P. Walsh, J. Electron. Mater. 28 (1999) L1.
- [7] M.S. Dresselhaus, Yu-Ming Lin, T. Koga, S.B. Cronin, O. Rabin, M.R. Black, G. Dresselhaus, in: T.M. Tritt (Ed.), Semiconductors and Semimetals: Recent Trends in Thermoelectric Materials Research III, Academic Press, San Diego, CA, 2001, p. 1.
- [8] Yu.I. Ravich, B.A. Efimova, I.A. Smirnov, Semiconducting Lead Chalcogenides, Plenum Press, New York, 1970.
- [9] G.D. Mahan, Solid State Phys. 51 (1997) 81.
- [10] Z. Dashevsky, L. Dudkin, J. Thermoelectr. 1 (1993) 93.
- [11] G. Springholz, V. Holy, M. Pinczolis, G. Bauer, Science 282 (1998) 734.
- [12] T.C. Harman, P.J. Taylor, D.L. Spears, M.P. Walsh, in: G. Chen, T. Tritt, T. Caillat (Eds.), Proceedings of the 18th International Conference on Thermoelectrics Baltimore, USA, August 29–September 2, 1999, IEEE, Piscataway, NJ, 1999, p. 280.
- [13] N.H. Abrikosov, L.E. Shelimova, Semiconducting Materials Based on A^4B^6 Compounds, Nauka, Moscow, 1975 (in Russian).
- [14] A.V. Lyubchenko, E.A. Sal'kov, F.F. Sizov, Physical Foundations of Semiconductor Quantum Photoelectronics, Naukova Dumka, Kiev, 1984.
- [15] J.N. Zemel, J.D. Jensen, R.B. Schoolar, Phys. Rev. 140 (1965) 330.
- [16] A. Nishiyama, J. Phys. Soc. Jpn. 40 (1976) 471.
- [17] S. Santhanam, A.K. Chaudhuri, Phys. Status Solidi, A Appl. Res. 83 (1984) K77.
- [18] P. Gonjaly, J.A. Agapito, D. Pardo, J. Phys. C. 19 (1986) 3619.
- [19] N. Ganesan, V. Sivaramakrishnan, Phys. Status Solidi, A Appl. Res. 105 (1988) 461.
- [20] E.H.C. Parker, D. Williams, Solid-State Electron. 20 (1977) 567.
- [21] D.V. Damodara, B.K. Seetharama, Thin Solid Films 116 (1984) 201.
- [22] E.I. Rogacheva, I.M. Krivulkin, O.N. Nashchekina, A.Yu. Sipatov, V.V. Volobuev, M.S. Dresselhaus, Appl. Phys. Lett. 78 (2001) 3238.
- [23] A.I. Fedorenko, O.N. Nashchekina, B.A. Savitskii, L.P. Shpakovskaya, O.A. Mironov, M. Oszwaldowski, Vacuum 43 (1992) 1191.
- [24] A. Ishido, M. Aoki, H. Fujiasu, J. Appl. Phys. 50 (1985) 1901.
- [25] O.A. Mironov, S.V. Chistyakov, I.Yu. Skrylov, A.I. Fedorenko, A.Yu. Sipatov, B.A. Savitskii, L.P. Shpakovskaya, O.N. Nashchekina, M. Oszwaldowski, Superlattices Microstruct. 8 (1990) 361.
- [26] G. Springholz, in: D. Khokhlov (Ed.), Lead Chalcogenides: Physics and Applications, Taylor and Francis, New York, 2002, p. 124.
- [27] I. Markov, S. Stoyanov, Contemp. Phys. 28 (1987) 267.
- [28] E.I. Rogacheva, O.N. Nashchekina, S.N. Grigorov, M.A. Us, M.S. Dresselhaus, S.B. Cronin, Nanotechnology 14 (2003) 53.
- [29] V.M. Kosevich, V.M. Ievlev, L.S. Palatnik, A.I. Fedorenko, Structure of Intercrystalline and Interphase Boundaries, Metalurgiya, Moscow, 1980 (in Russian).
- [30] A.I. Fedorenko, B.A. Savitskii, A.Yu. Sipatov, L.P. Shpakovskaya, Kristallografia 27 (1982) 948.
- [31] A.V. Golubkov, E.V. Goncharova, V.P. Zhuze, G.M. Loginov, V.M. Sergeeva, I.A. Smirnov, Physical Properties of Chalcogenides of Rare-Earth Elements, Nauka, Leningrad, 1973 (in Russian).
- [32] W.A. Jesser, D. Kuhlmann-Wilsdorf, Phys. Status Solidi 19 (1967) 95.
- [33] R.L. Petritz, Phys. Rev. 110 (1958) 1256.
- [34] O.N. Nashchekina, E.I. Rogacheva, L.P. Shpakovskaya, V.I. Pinegin VI, A.I. Fedorenko, Mater. Res. Soc. Symp. Proc. 378 (1995) 255.
- [35] E.I. Rogacheva, T.V. Tavrina, O.N. Nashchekina, V.V. Volobuev, A.G. Fedorov, A.Yu. Sipatov, M.S. Dresselhaus, Thin Solid Films 423 (2003) 257.
- [36] E.I. Rogacheva, I.M. Krivulkin, O.N. Nashchekina, A.Yu. Sipatov, V.V. Volobuev, M.S. Dresselhaus, Appl. Phys. Lett. 78 (2001) 1661.